Effects of Storage Pressure and Temperature on the Volume and Mass of a Two-Tank Inventory System for Marine sCO_2 Brayton Cycles

Jeong Min Baek [a], Jeong Ik Lee [a*]
[a]*Dept. Nuclear & Quantum Eng., KAIST, 291 Daehak-ro, Yuseong-Gu, Daejeon 34141, Republic of Korea*
[*]*Corresponding author: jeongiklee@kaist.ac.kr*

Keywords : sCO_2 Brayton cycle, Inventory control, Two-tank inventory system, Nuclear marine propulsion

1. Introduction

As decarbonization requirements for international shipping continue to strengthen, the International Maritime Organization (IMO) aims to achieve net-zero greenhouse gas (GHG) emissions by around 2050 [1]. In this context, nuclear propulsion is being considered as a promising alternative to conventional fossil-fuel-based propulsion systems [2]. Among various power conversion systems, the supercritical carbon dioxide (sCO_2) Brayton cycle has been investigated as a promising option for nuclear-powered ships because of its high thermal efficiency and compactness. In actual marine operation, propulsion power demand continuously varies with operating conditions, and the sCO_2 cycle must therefore be capable of stable operation over a wide load range. Accordingly, various part-load control strategies have been investigated [2], among which inventory control is considered a major strategy because it can regulate cycle output by adjusting the CO_2 inventory with a relatively small efficiency penalty [3].

Implementing inventory control in an actual system requires tanks to supply CO_2 to the cycle or store CO_2 removed from the cycle. In marine applications, limited onboard space and system mass are major design constraints, and therefore the size and mass of the inventory tanks must be considered together. Even for the same required CO_2 transfer mass, the required storage volume and structural requirements of the pressure vessel can vary with storage temperature and pressure, resulting in changes in the external volume and total mass of the tank. Therefore, marine inventory tank design should consider not only the required CO_2 storage capacity but also the effects of storage temperature and pressure on the pressure-vessel size and mass.

Previous studies have mainly investigated the effects of initial tank conditions and finite storage capacity on the operating range and dynamic characteristics of inventory control [4–6], or estimated the required internal volume based on CO_2 inventory changes and storage temperature under prescribed storage-pressure conditions [7, 8]. In contrast, studies that consider storage pressure and temperature as design variables and evaluate the size and mass of the pressure vessel, including its structure, remain limited. Therefore, for marine applications with strict onboard space and mass constraints, the sizing characteristics of inventory tanks under different storage conditions need to be evaluated.

Accordingly, this study evaluates the effects of storage pressure and temperature on the size and mass of a two-tank inventory system consisting of a high-pressure supply tank (HP tank), which supplies CO_2 to the cycle, and a low-pressure receiver tank (LP tank), which stores CO_2 removed from the cycle. Based on the part-load operating results of a previously analyzed molten chloride fast reactor (MCFR)–sCO_2 marine propulsion system [9], sizing analyses were performed for the HP and LP tanks. The maximum storage pressure was used as the pressure variable for both tanks, corresponding to the state before CO_2 supply to the cycle for the HP tank and after CO_2 recovery from the cycle for the LP tank, each under three storage-temperature conditions. For each condition, the external volume of the pressure vessel, including the structural thickness, was calculated, and the total mass was determined by considering both the structural mass and the CO_2 mass contained in the tank. The results are intended to provide sizing trend for a two-tank inventory system for marine applications where onboard space and mass are constrained.

2. Methodology

2.1 Reference System and Inventory Configuration

In this study, the part-load operating results of the MCFR–sCO_2 marine propulsion system analyzed by Baek et al. [9] were used as the reference conditions. Based on the variations in the cycle inventory and pressures according to the inventory control results, the required CO_2 transfer mass and pressure conditions for the inventory tanks were determined.

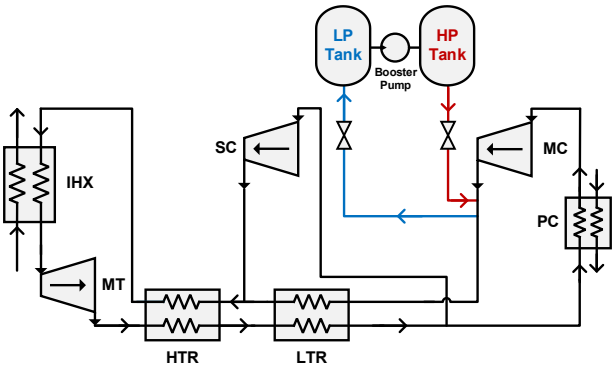


Fig. 1. Reference MCFR–sCO_2 marine propulsion system and two-tank inventory configuration

Figure 1 shows the reference MCFR–sCO_2 system and the two-tank inventory configuration considered in this study. Various inventory configurations can be arranged depending on the connection locations between the inventory tank and the cycle. In configurations where CO_2 is injected into the low-pressure side at the compressor inlet and extracted from the high-pressure side at the compressor outlet, Oh and Lee [10] pointed out that supplying CO_2 to the compressor inlet causes the mass flow rate and power requirement of the compressor to increase before those of the turbine, which can delay the power response. Considering the operational characteristics of marine propulsion systems that require rapid load control responses [11], this study considered a control scheme in which both CO_2 injection and extraction are performed at the main-compressor (MC) outlet on the high-pressure side.

When both injection and extraction are performed at the MC outlet, both single-tank and two-tank configurations are conceptually applicable. However, in a single-tank configuration, if immediate injection is required after CO_2 extraction from the cycle, the stored CO_2 must be pressurized using a device such as a booster pump to exceed the MC outlet pressure, making it difficult to respond rapidly to power changes. In contrast, a two-tank configuration allows the HP tank to be pre-pressurized above the MC outlet pressure, enabling immediate CO_2 injection by pressure difference. Accordingly, this study adopted the two-tank configuration consisting of an HP tank maintained above the MC outlet pressure and an LP tank maintained at a lower pressure, and established the allowable storage pressure boundaries for each tank based on the MC outlet pressure across the entire part-load operating range.

2.2 Inventory Requirement and Tank Conditions

The required CO_2 transfer mass for the HP and LP tanks was determined from the reference part-load operating results. Figure 2 illustrates the corresponding cycle inventory variation over this range.

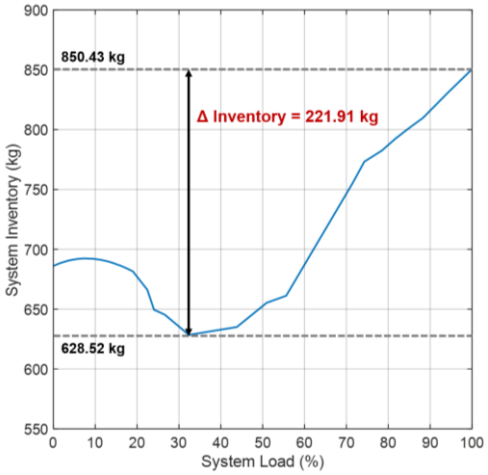


Fig. 2. CO_2 inventory variation in the reference cycle during part-load operation

Similar to previous sCO_2 inventory tank studies [8], the required CO_2 transfer mass was determined from the difference between the maximum and minimum cycle inventories, which was 221.91 kg in this study. Accordingly, the HP tank was sized to supply up to 221.91 kg of CO_2 to the cycle, while the LP tank was sized to receive the same amount of CO_2 from the cycle.

Next, the cycle-side pressure variation at the MC outlet was analyzed to establish the storage-pressure ranges for both HP and LP tanks. Figure 3 shows the MC outlet pressure variation over the full part-load operating range.

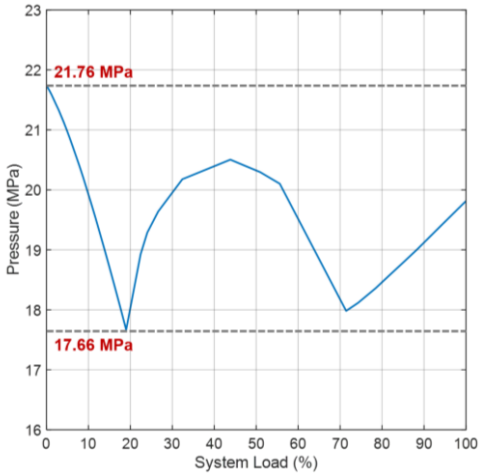


Fig. 3. Pressure Variation at the MC outlet

Based on the pressure variations over the full part-load operating range, the most restrictive cycle-side pressure was used to establish the pressure condition for each tank. In addition, a minimum driving pressure difference of 0.5 MPa between each tank and the MC outlet was assumed to provide the pressure difference required for CO_2 transfer.

For the HP tank, the minimum storage pressure after CO_2 supply was fixed at 22.26 MPa based on the maximum MC outlet pressure of 21.76 MPa and the assumed driving pressure difference of 0.5 MPa. The maximum storage pressure before CO_2 supply was treated as an analysis variable and varied from 23 to 32 MPa. For the LP tank, the minimum storage pressure before CO_2 recovery was fixed at 8 MPa. The maximum storage pressure after CO_2 recovery was treated as an analysis variable and varied from 9 to 17 MPa, remaining below the allowable upper limit of 17.16 MPa determined from the minimum MC outlet pressure of 17.66 MPa and the required driving pressure difference.

In addition to storage pressure, three storage temperatures of 20, 40, and 60 ℃ were considered for both the HP and LP tanks to evaluate the effect of storage temperature on tank sizing. An isothermal process was assumed during CO_2 supply or recovery, and the thermal-management duty required to maintain the prescribed storage temperature was not considered in the present analysis. The pressure and temperature analysis conditions are summarized in Table I.

Table I: Analysis conditions for inventory tank sizing

Parameter	HP tank	LP tank
Pressure variable	Maximum storage pressure	Maximum storage pressure
Pressure range (MPa)	23.0 – 32.0	9.0 – 17.0
Storage temperature (℃)	20 / 40 / 60	20 / 40 / 60

2.3 Internal Volume Estimation

Previous sCO_2 inventory tank studies estimated the required storage volume using the CO_2 transfer mass and the density difference between the initial and final storage states [7, 8]. Following the same approach, the required internal volumes of the HP and LP tanks were calculated using the CO_2 transfer mass and storage conditions established in Section 2.2. Each tank was assumed to be a rigid vessel with a constant internal volume, and the CO_2 density at each storage state was calculated using NIST REFPROP [12].

For the HP tank, the CO_2 density decreases from the state at the maximum storage pressure to that at the minimum storage pressure as CO_2 is supplied to the cycle, whereas for the LP tank, the density increases from the state at the minimum storage pressure to that at the maximum storage pressure as CO_2 is received from the cycle. For both tanks, the required internal volume was calculated using Equation (1) based on the required CO_2 transfer mass and the density difference between the states at the maximum and minimum storage pressures.

$$V = \frac{\Delta m_{CO_2}}{\rho_{max} - \rho_{min}} \tag{1}$$

In Equation (1), Δm_{CO_2} denotes the required CO_2 transfer mass of 221.91 kg determined in Section 2.2, while ρ_{max} and ρ_{min} denote the CO_2 densities at the maximum and minimum storage pressures, respectively. Equation (1) was applied to all storage pressure and temperature conditions listed in Table I to calculate the required internal volumes of the HP and LP tanks.

2.4 Pressure Vessel Sizing

To translate the required internal volumes estimated in Section 2.3 into actual pressure-vessel dimensions, the basic vessel geometry was first established. Jeong et al. [13] employed a pressure vessel consisting of a cylindrical section and 2:1 ellipsoidal heads for compressed CO_2 storage and applied a height-to-diameter ratio of 4:1. Based on this configuration, the same basic vessel geometry was adopted in the present study, with the cylindrical-section length set to four times the inner diameter and the internal depth of each ellipsoidal head set to one-fourth of the inner diameter.

Figure 4 shows the pressure-vessel geometry based on these geometric ratios and the major parameters used in the subsequent sizing calculations. Here, D_i and R_i denote the inner diameter and inner radius of the cylindrical section, respectively, while L_c and h_h denote the cylindrical-section length and the internal depth of the ellipsoidal head, respectively. In addition, t_s and t_h denote the wall thickness of the cylindrical shell and ellipsoidal head, respectively.

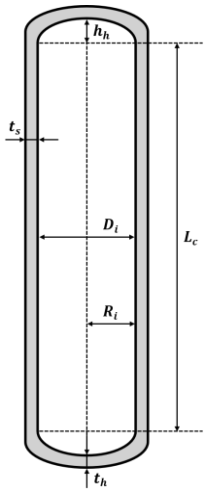


Fig. 4. Geometry and geometric parameters of the inventory tank pressure vessel

Based on the prescribed vessel geometry, the required internal volume estimated in Section 2.3 can be expressed as the sum of the cylindrical-section volume and the volumes of the two ellipsoidal heads, as given in Equation (2).

$$V_{int} = \pi R_i^2 L_c + \frac{4}{3}\pi R_i^2 h_h \tag{2}$$

For each storage condition, the required internal volume obtained in Section 2.3 was applied to Equation (2), and D_i , L_c , and h_h were determined while maintaining the prescribed geometric ratios.

After determining the internal vessel dimensions, the wall thicknesses required to withstand the storage pressure were calculated. Based on ASME BPVC Section VIII, Division 1 [14], the required wall thicknesses of the cylindrical shell and the 2:1 ellipsoidal head were calculated using Equations (3) and (4), respectively.

$$t_s = \frac{PR_i}{SE - 0.6P} \tag{3}$$

$$t_h = \frac{PD_i}{2SE - 0.2P} \tag{4}$$

For P in Equations (3) and (4), the maximum storage pressure experienced by each tank during CO_2 transfer was used. Accordingly, this corresponded to the storage pressure before CO_2 supply for the HP tank and after CO_2 recovery for the LP tank.

Next, the pressure-vessel material was selected to determine the material properties required for the wall-thickness calculation. SA-516 Grade 70, specified in ASME BPVC Section II, Part A [15] as a carbon-steel pressure-vessel plate, was selected in this study.

According to ASME BPVC Section II, Part D [16], the maximum allowable stress of 138 MPa was applied at the three storage temperatures of 20, 40, and 60 ℃. In addition, the weld joint efficiency was set to 1.0 assuming fully radiographed butt-welded joints, and a material density of 7,850 kg/m^3 was used for the structural-mass calculation. The major geometric and material parameters used for pressure-vessel sizing are summarized in Table II.

Table II: Pressure vessel sizing parameters

Parameter	Value
Cylindrical length-to-diameter ratio	4.0
Head depth-to-diameter ratio	0.25
Material	SA-516 Grade 70
Maximum allowable stress, S (MPa)	138
Weld joint efficiency, E (-)	1.0
Material density, ρ_{mat} (kg/m^3)	7,850

Using the pressure-vessel dimensions and wall thicknesses determined above, the external volume and structural mass were evaluated for each sizing condition. The external geometry of the ellipsoidal heads was assumed to maintain the same 2:1 ratio as the internal geometry, and the external volume of the pressure vessel, including the cylindrical shell and two ellipsoidal heads, was calculated using Equation (5).

$$V_{ext} = \frac{\pi}{4}(D_i + 2t_s)^2 L_c + \frac{\pi}{12}(D_i + 2t_h)^3 \qquad (5)$$

The structural mass of the pressure vessel was calculated from the material density and the difference between the external and internal volumes. To evaluate the total mass of each tank, the internal CO_2 mass was added to the structural mass at the maximum storage pressure, which corresponds to the state before CO_2 supply for the HP tank and after CO_2 recovery for the LP tank. This sizing procedure was applied to all storage pressure and temperature conditions listed in Table I to determine the external volume and total mass. The effects of these storage conditions on tank sizing are compared in the following sections.

3. Tank Volume and Mass Evaluation Results

3.1 Required Internal Volume

Although both the HP and LP tanks are connected to the MC outlet, different storage pressure ranges are imposed on each tank. Figures 5 and 6 show the required internal volume results for the HP and LP tanks according to storage pressure and temperature, respectively. For both tanks, increasing the storage pressure expands the CO_2 density difference before and after mass transfer, thereby continuously reducing the required internal volume. This occurs because the required internal volume to accommodate a given transfer mass is directly governed by the density variation formed within the operating pressure range rather than the absolute density at a specific state.

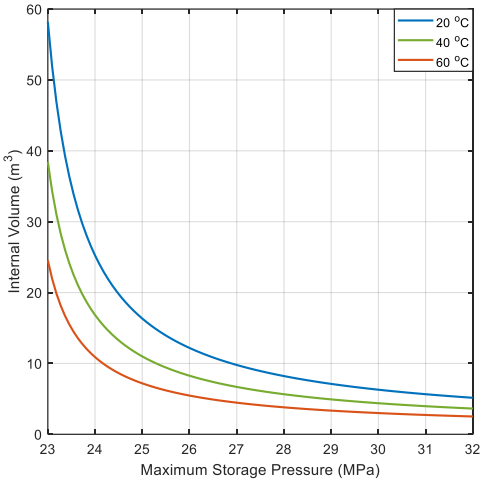


Fig. 5. Required internal volume of the HP tank according to maximum storage pressure and storage temperature

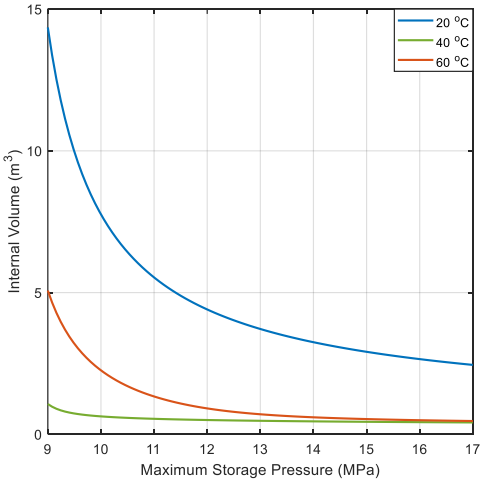


Fig. 6. Required internal volume of the LP tank according to maximum storage pressure and storage temperature

However, owing to the difference in operating pressure ranges between the two tanks, the optimal storage temperature and the volume reduction behavior with respect to pressure increase were evaluated differently. For the HP tank shown in Figure 5, under the condition where the minimum storage pressure is fixed at 22.26 MPa, the 60 ℃ condition produced the largest density variation within its operating pressure range and recorded the smallest internal volume, followed by 40 ℃ and 20 ℃.

In contrast, for the LP tank shown in Figure 6 under the condition where the minimum storage pressure is fixed at 8 MPa, the 40 ℃ condition achieved the smallest internal volume unlike the HP tank. Under the 40 ℃ condition, a relatively large density difference was already formed in the lower maximum storage pressure region. Consequently, as the maximum storage pressure further increased, the additional volume reduction rate decreased rapidly and the curve became gradually flattened in the high-pressure region. Conversely, under the 20 ℃ and 60 ℃ conditions, the volume reduction

effect with increasing maximum storage pressure persisted over a wider pressure range.

3.2 Pressure Vessel Wall Thickness

The required wall thickness of the pressure vessels was calculated using the derived internal volume results. Figures 7 and 8 display the required wall thickness of the HP and LP tanks according to storage pressure and temperature respectively.

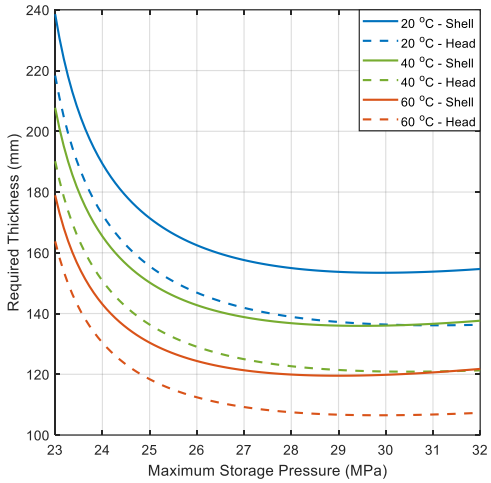


Fig. 7. Required wall thickness of the HP tank according to maximum storage pressure and storage temperature

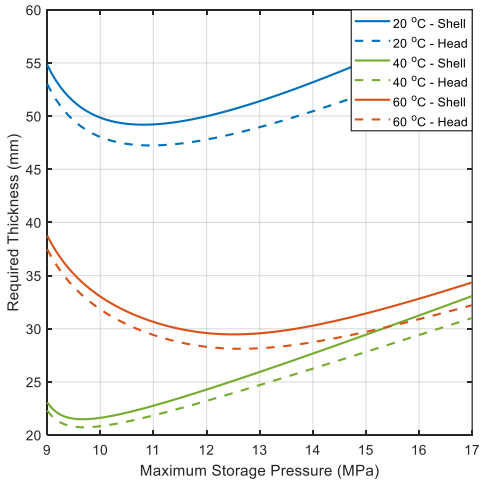


Fig. 8. Required wall thickness of the LP tank according to maximum storage pressure and storage temperature

Generally, under a constant volume condition, a higher storage pressure increases the pressure loading and thus requires a thicker wall. However, in the present sizing evaluation, both the required internal volume and vessel radius decrease simultaneously as the storage pressure increases. Consequently, the wall thickness of both tanks exhibited a common non-monotonic behavior where it decreased and then increased. In the low pressure range, the required internal volume is extremely large and results in a large vessel radius, which demands a thick wall. As the storage pressure increases, the structural benefit from the reduced vessel radius outweighs the effect of increased pressure loading in the lower pressure region and leads to a decrease in wall thickness. In the higher pressure region, however, the rate of internal volume reduction attenuates and diminishes the advantage of vessel radius reduction, whereas the influence of increased pressure loading becomes dominant and causes the wall thickness to increase again.

Despite this common behavior, the transition point where the wall thickness begins to increase again varied depending on the operating pressure range and density variation characteristics of each tank. For the HP tank, the required wall thickness decreased sharply as the maximum storage pressure increased and then gradually increased above a certain pressure. In contrast, for the LP tank, especially under the 40 ℃ condition, most of the internal volume reduction occurred at lower maximum storage pressures and additional volume reduction at higher pressures was marginal. Accordingly, the benefit of vessel radius reduction diminished rapidly, and the effect of increasing pressure loading became dominant at a relatively low maximum storage pressure, causing the wall thickness to increase earlier.

3.3 External Volume Characteristics

The external volume representing the actual physical space occupied by the pressure vessel on board was evaluated by incorporating both the required internal volume and the structural wall thickness. Figures 9 and 10 display the external volume results for the HP and LP tanks according to storage pressure and temperature respectively. Within the present analyzed pressure range, the reduction in internal volume and vessel diameter acted more dominantly than the increase in wall thickness for both tanks. Consequently, the external volumes of both tanks exhibited a common trend of continuous decrease as the storage pressure increased.

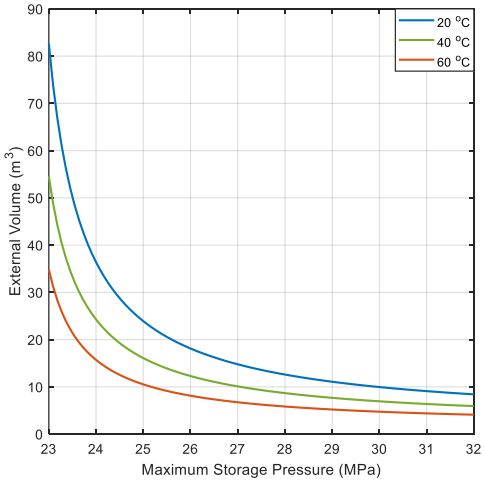


Fig. 9. External volume of the HP tank according to maximum storage pressure and storage temperature

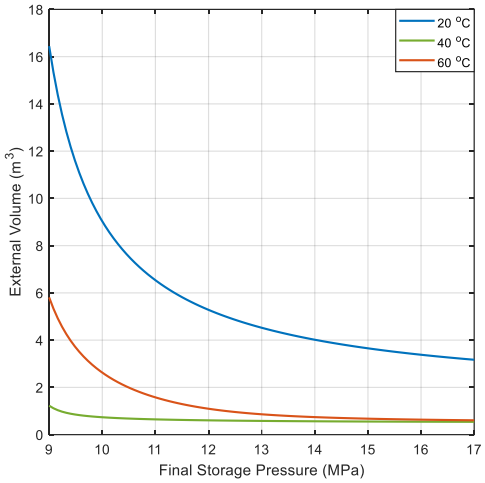


Fig. 10. External volume of the LP tank according to maximum storage pressure and storage temperature

Consistent with the internal volume results, the smallest external volume was recorded at 60 ℃ for the HP tank and at 40 ℃ for the LP tank. Although increasing the storage pressure is effective in reducing the external volume, the additional volume reduction for a given pressure increase gradually diminished toward the higher pressure region.

3.4 Total Mass and Storage Condition Characteristics

To evaluate the onboard weight constraints of marine propulsion systems, the total mass was analyzed by combining the structural mass of the pressure vessel and the fluid mass of the stored CO_2. Figure 11 presents the total mass results of the HP tank according to storage pressure and temperature.

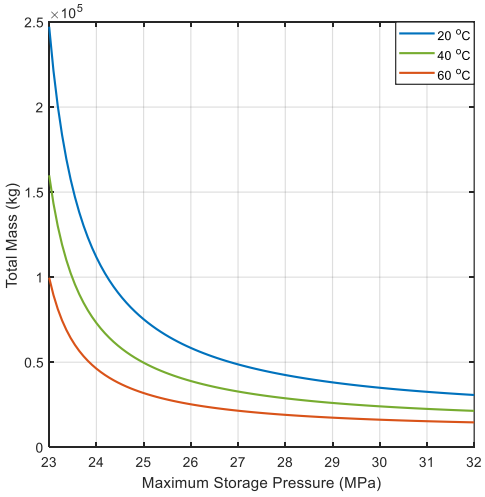


Fig. 11. Total mass of the HP tank according to maximum storage pressure and storage temperature

Over the entire analyzed pressure range from 23 to 32 MPa, the total mass of the HP tank continuously decreased as the maximum storage pressure increased. This occurs because the required internal volume decreases with a higher maximum storage pressure, which significantly reduces the stored CO_2 fluid mass. Within the analyzed pressure range, the mass reduction benefit resulting from internal volume reduction was dominant, leading to a continuous decrease in total mass with the reduction rate becoming gradually flattened in the high-pressure region. Across all investigated conditions, the HP tank recorded its lowest total mass under the 60 ℃ condition.

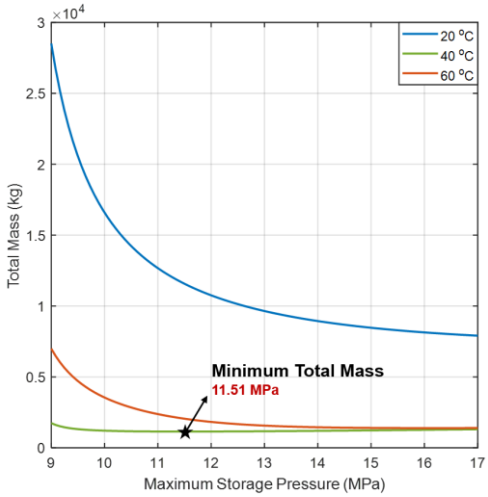


Fig. 12. Total mass of the LP tank according to maximum storage pressure and storage temperature

Figure 12 presents the total mass results of the LP tank according to storage pressure and temperature. The LP tank exhibited a clear non-monotonic trend where the total mass decreased and then increased with increasing storage pressure. Among all storage temperature conditions, the 40 ℃ condition yielded the lowest total mass within the analyzed pressure range. Specifically at 40 ℃, the total mass decreased as the maximum storage pressure increased, reached a distinct minimum at a maximum storage pressure of 11.51 MPa, and then slightly increased. This result is attributed to a clear trade-off between the mass reduction gained from internal volume and vessel radius reduction and the structural mass penalty caused by increased wall thickness. Prior to 11.51 MPa, the mass reduction benefit from internal volume reduction was dominant. Beyond 11.51 MPa, however, the internal volume reduction effect saturated while the structural mass penalty caused by increased wall thickness surpassed the volume benefit.

Similar to the mechanism observed in the LP tank, increasing the maximum storage pressure of the HP tank beyond 32 MPa may eventually yield a total mass minimum as the volume reduction benefit attenuates and structural burden grows. However, excessively raising the storage pressure to secure the minimum mass is not always desirable. In the high-pressure region, as confirmed by the present results, the additional reduction in volume and mass for a pressure increase becomes very small, while inducing severe design burdens on high-pressure components including tank-side connecting

piping, valves, and booster systems as well as increasing the structural thickness of the tank itself.

Overall, these evaluation results clearly demonstrate that the storage pressure and temperature of inventory tanks are key design variables that dictate volume and mass characteristics rather than mere operating boundary conditions. Therefore, in designing an actual marine sCO_2 inventory system, rather than simply raising the storage pressure or uniformly applying a specific temperature, it is necessary to select storage conditions suitable for the spatial and weight constraints of the target system by comprehensively considering both the limitations of volume and mass reduction and the pressure-related structural burden within the operating pressure range of each tank.

4. Summary and Conclusions

In this study, the effects of storage pressure and temperature on the physical size and total mass of a two-tank inventory system were evaluated for a marine sCO_2 nuclear propulsion system. Based on the part-load operating characteristics of the MCFR–sCO_2 marine propulsion system, sizing analyses were performed for the HP and LP tanks under various pressure ranges and representative storage temperatures of 20, 40, and 60 ℃.

The analysis revealed that for both tanks, the required internal volume continuously decreased as the maximum storage pressure increased. However, due to the different operating pressure ranges imposed on each tank, the temperature yielding the smallest required volume among the investigated conditions differed as 60 ℃ for the HP tank and 40 ℃ for the LP tank. These temperature conditions that minimized the volume were also confirmed to produce the lowest total mass for each tank within the analyzed temperature set. Regarding the total mass behavior with respect to maximum storage pressure, the total mass of the HP tank continuously decreased up to the maximum analyzed storage pressure of 32 MPa under 60 ℃. Conversely, the LP tank exhibited a clear trade-off between internal volume reduction and structural mass penalty under 40 ℃, reaching a distinct minimum total mass at a maximum storage pressure of 11.51 MPa.

These evaluation results demonstrate that the storage pressure and temperature of inventory tanks are crucial design variables that dictate the overall spatial and weight footprints rather than mere operating boundary conditions. Therefore, designing inventory tanks for space-constrained and mass-constrained marine propulsion systems requires a comprehensive approach that considers total mass trends and pressure-related structural burdens together with physical volume reduction. As future work, the thermal behavior of the inventory tanks during CO_2 transfer will be evaluated beyond the present isothermal assumption, including the thermal-management duty and associated auxiliary power required to maintain the prescribed storage temperature.

ACKNOWLEDGEMENT

This work was supported by the National Research Foundation of Korea(NRF) grant funded by the Korea government(MSIT) (No. RS-2025-25454059).

REFERENCES

[1] International Maritime Organization, “2023 IMO Strategy on Reduction of GHG Emissions from Ships,” *Resolution MEPC.377(80)*, 2023.

[2] Z. Li, M. Shi, Y. Shao, and W. Zhong, “Supercritical CO_2 Cycles for Nuclear-Powered Marine Propulsion: Preliminary Conceptual Design and Off-Design Performance Assessment,” *Journal of Thermal Science*, Vol. 33, pp. 328–347, 2024.

[3] S.S. Gupta and P. Kumar, “Optimal Part-Load Performance of Supercritical Carbon Dioxide Brayton Cycles During Inventory Control,” *Journal of Engineering for Gas Turbines and Power*, Vol. 147, 051023, 2025.

[4] J.J. Lee, B.S. Oh, J.Y. Baek, and J.I. Lee, “Preliminary Study on Tank Design for S-CO_2 Power Cycle Inventory Control,” *Transactions of the Korean Nuclear Society Autumn Meeting*, 2019.

[5] M. Marchionni, M. Usman, L. Chai, and S.A. Tassou, “Inventory Control Assessment for Small Scale sCO_2 Heat to Power Conversion Systems,” *Energy*, Vol. 267, 126537, 2023.

[6] M. Marchionni, G. Bianchi, and S.A. Tassou, “Dynamics of sCO_2 Heat-to-Power Units Equipped with Dual Tank Inventory Control System,” *Proceedings of the 6th International Seminar on ORC Power Systems*, Paper 129, 2021.

[7] B. Tom, J. Smith, and M.D. Towler, “Inventory Management Operational Strategies for a 10 MWe sCO_2 Power Block,” *Proceedings of the 7th International Supercritical CO_2 Power Cycles Symposium*, Paper 104, 2022.

[8] H.Y. Ye, J. Hong, D. Kim, Y. Jung, S. Choi, and J. Eoh, “Storage Tank Design and Dynamic Analysis of sCO_2 Power Conversion System for Thermal Energy Storage System,” *Transactions of the Korean Nuclear Society Spring Meeting*, 2024.

[9] J.M. Baek, G. Kim, S. Lee, S. Choi, and J.I. Lee, “Development of Supercritical CO_2 Power System Control for Preventing Coolant-Salt Solidification in MCFR for Marine Propulsion,” *Nuclear Engineering and Design*, Vol. 457, 115090, 2026.

[10] B.S. Oh and J.I. Lee, “Study of Autonomous Control System for S-CO_2 Power Cycle,” *Proceedings of the 3rd European Supercritical CO_2 Conference*, pp. 345–352, 2019.

[11] J.Y. Baek, J.J. Lee, and J.I. Lee, “Transient Analysis of the Super-Critical Carbon Dioxide Cycle Coupled to Pressurized Water Reactor for Nuclear Powered Ships,” *Proceedings of the 4th European sCO_2 Conference for Energy Systems*, 2021.

[12] E.W. Lemmon, I.H. Bell, M.L. Huber, and M.O. McLinden, “REFPROP, Version 10.0,” *NIST Standard Reference Database 23*, 2018.

[13] Y. Jeong, Y.J. Chae, S. Lee, and J.I. Lee, “Effect of High Pressure Vessel Size on Compressed CO_2 Energy Storage for Nuclear Power Plant to Complement Renewable Energy,” *Transactions of the Korean Nuclear Society Virtual Spring Meeting*, 2020.

[14] ASME, *Boiler and Pressure Vessel Code, Section VIII, Division 1*, 2025.

[15] ASME, *Boiler and Pressure Vessel Code, Section II, Part A*, 2025.

[16] ASME, *Boiler and Pressure Vessel Code, Section II, Part D*, 2025.